European Journal of Radiology Open 9 (2022) 100410

Contents lists available at ScienceDirect

European Journal of Radiology Open

journal homepage: www.elsevier.com/locate/ejro

3D isotropic spine echo MR imaging of elbow: How it helps surgical decisions

Bayan Mogharrabi [a], Alison Cabrera [b], Avneesh Chhabra [a,b,c,*]

[a] Department of Radiology at UT Southwestern Medical Center, USA
[b] Department of Orthopedic Surgery at UT Southwestern Medical Center, USA
[c] Adjunct faculty- Johns Hopkins University, USA & Walton center of neurosciences, UK

ARTICLE INFO

Keywords:
Elbow
MRI
3-dimensional
2-dimensional
Surgery

ABSTRACT

Elbow derangements are common. Clinical examination is supplemented by magnetic resonance imaging (MRI) for optimal diagnostic assessment of such disorders. 3-dimensional (3D) imaging is feasible on newer MR scanners in acceptable acquisition times. Isotropic high-resolution 3D MRI affords multiplanar reconstructions and aids in diagnostic evaluation of elbow disorders and pre-/post-surgical assessments. The article details technical considerations of 3D elbow MRI and discusses its role in diagnostic evaluation of elbow disorders with relevant comparisons to 2D MRI and emphasizes as to how such advanced imaging assists in pre- and post-surgical assessments of tendon and ligament derangements.

1. Introduction

Elbow pain, instability, and dysfunction are common and occur at all ages. These symptoms are caused by a wide variety of pathologies including repeated microtrauma or acute injury, and the treatment options range from conservative therapy to surgery [1]. Initial diagnostic evaluation includes screening radiographs in orthogonal (anteroposterior and lateral) views. The radiographs allow evaluation of bony hypertrophy and/or cystic changes at sites of epicondylitis and tendinopathy, visualization of soft tissue swelling, bony injuries, calcifications, and importantly, joint effusion and bursitis [2]. Ultrasound (US) affords real-time assessment of joint effusion, bursitis, tendinopathy, tears, and soft tissues around the elbow [3]. Computed tomography is used for further characterization of elbow bony injury and hardware complications. MR imaging is the best comprehensive imaging modality for assessing the whole spectrum of intra- and extra-articular elbow pathologies as it offers excellent spatial resolution and soft tissue and bone marrow contrast [2,4,5]. MR imaging of the elbow has been historically performed using surface coils and 2-D (dimensional) sequences with inter-slice gaps and 3.5–5 mm slice thickness [T2-weighted, (T2W), T1W, or intermediate weighted fast spin echo)] [6,7]. 3D imaging allows isotropic volume imaging at sub-1.0 mm resolutions for improved assessment of musculotendinous structures, ligament injuries, and osteochondral lesions [6].

This article reviews fundamental concepts for the evaluation of elbow pathologies on 3D isotropic MR imaging and authors discuss the key clinical perspectives with imaging correlations of 2D versus 3D imaging, and how the advanced imaging aids surgical decisions for optimal patient management.

2. Technical considerations of 3D MRI

Conventional MRI study can take up to 30 min to acquire multiplanar 2D imaging on the current high field scanners. The 2D MR imaging sequences are obtained with a 10–20% interslice gap and thicker slices, to the order of 3.5–5 mm depending upon the scanner capability. 2D MR imaging generates smoother appearing images but these obscure the fine soft tissue and bony details. In our tertiary care center, acquisition time is reduced to less than 12 min by using three-plane intermediate weighted T2W Dixon imaging and simultaneous generation of in-phase, opposed-phase, and water maps. Such imaging also allows marrow evaluation without additional need for T1W imaging [8]. Other disadvantages of 2D imaging include- potential bias and errors in positioning and acquisition by the technologist, partial volume artifacts, limited fluid-cartilage contrast at intermediate-weighted echo times, and inability to manipulate images in arbitrary planes along the axes of tissues of interest without causing significant stair-step artifacts (Fig. 1).

While the older 3D sequences were gradient-echo based and low

* Correspondence to: University of Texas at Southwestern Medical Center, 5323 Harry Hines Blvd, Dallas, TX 75390, USA.
E-mail address: Avneesh.Chhabra@UTSouthwestern.edu (A. Chhabra).

https://doi.org/10.1016/j.ejro.2022.100410
Received 4 October 2021; Received in revised form 1 February 2022; Accepted 23 February 2022

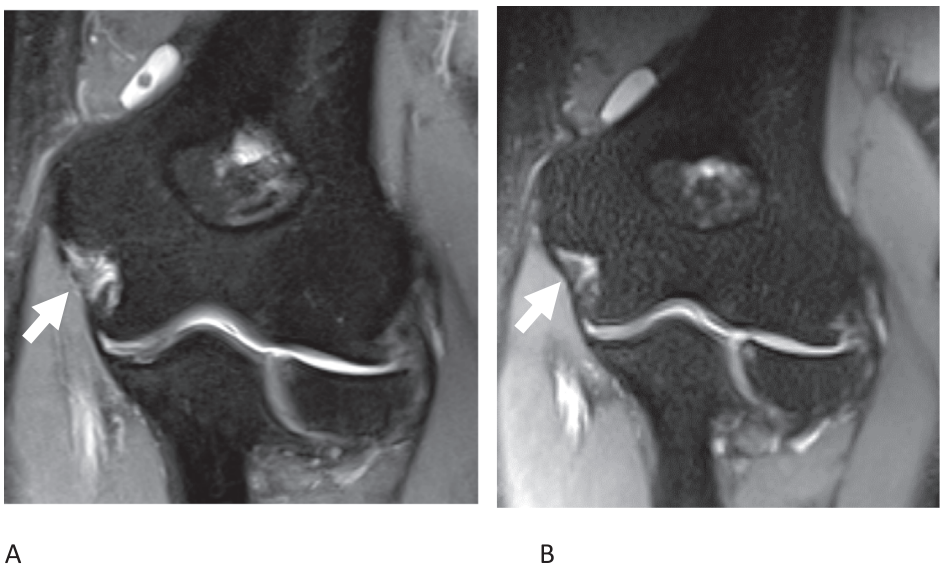

Fig. 1. 2D vs. 3D comparison. High-resolution spin echo 2D (a) and 3D (b) fat suppressed intermediate-weighted (fsIW) coronal images show similar bony resolution on both images. Notice better definition of ulnar collateral ligament (arrows) on 3D images due to mitigation of partial volume artifacts.

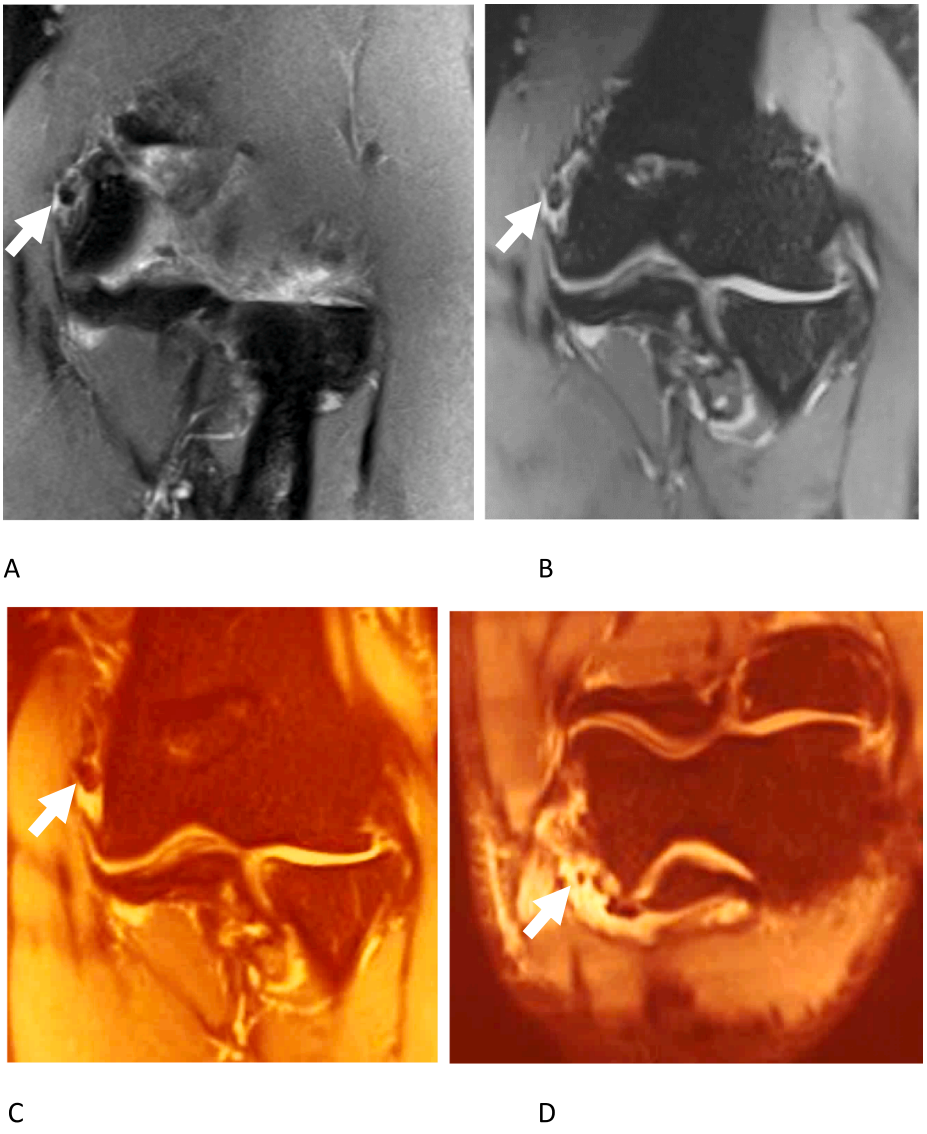

Fig. 2. 2D vs. 3D comparison- intra-articular bodies. High-resolution spin echo 2D (a) and 3D (b) fsIW coronal and heat map color-rendered images (c,d) show intra-articular body in posteromedial recess of joint (arrows). Notice additional small bodies on reconstructed axial 3D image (arrow).

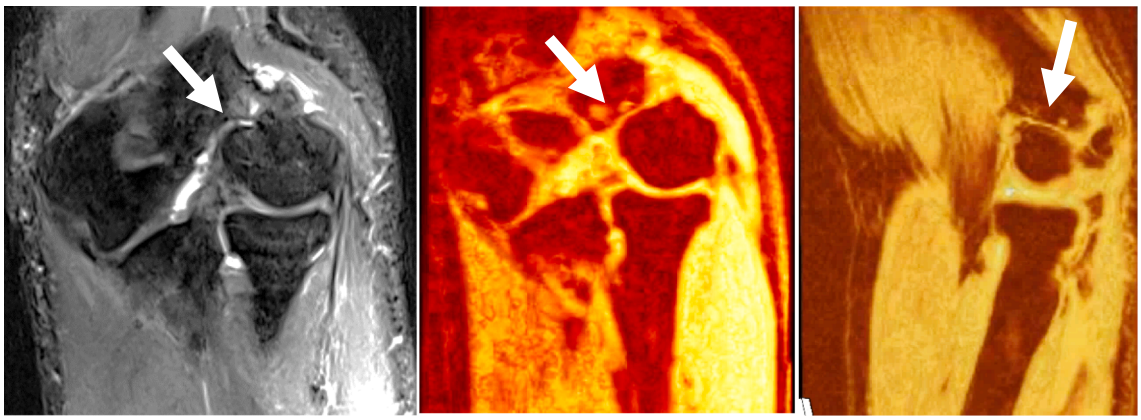

Fig. 3. Subacute distal humerus fracture-deformity with pseudoarthrosis. Coronal 2D (a) and coronal and sagittal 3D (b,c) images shows fracture deformity of radial sided metaphysis with extension into the inter-condylar area and pseudoarthrosis with subcortical cystic changes (arrows).

resolution, development of 3D turbo spin echo with variable flip angle evolutions, and partial Fourier sampling led to higher-resolution, isotropic, and faster 3D imaging [9]. 3D imaging currently can be obtained in 6 min or less due to software and hardware improvements and provides sub-1.0 mm isotropic resolution on 3 T (tesla) and newer 1.5 T scanners. 3D imaging renders excellent fluid-tissue contrast, great spatial resolution, mitigates the partial-voluming artifacts and susceptibility artifacts, and affords multiplanar reconstructions in any desired plane for improved visualization of tendon and ligament lesions (Fig. 1). As voxel size decreases, the graininess or noise in the images increases. In our practice, we find that 0.65–0.7 mm voxel results in superior signal to noise ratio for an average-sized patient and 0.7–0.8 mm for a larger patient with a reasonable scanning time under 6 min. Recent image acceleration techniques and advances include

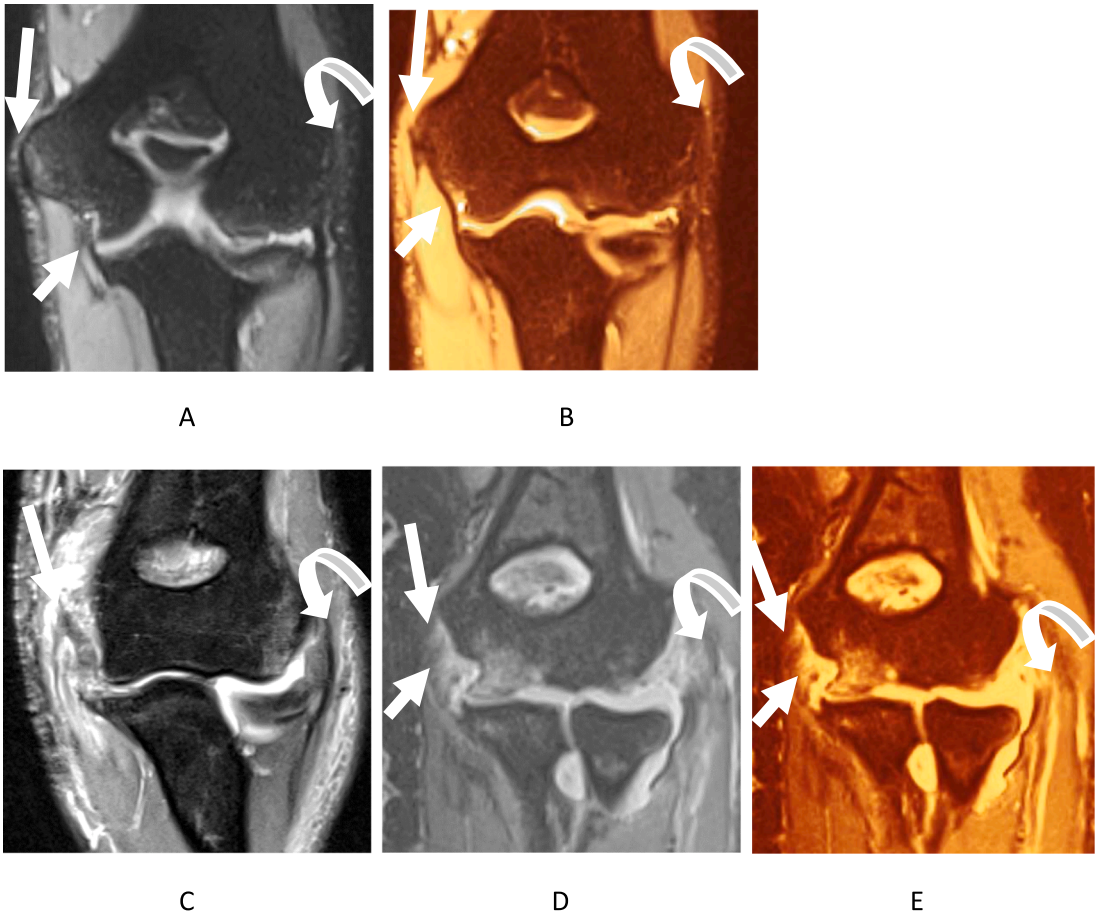

Fig. 4. Normal and abnormal UCL and elbow tendons. Coronal 3D (a) fsIW and heat map color-rendered (b) images show normal taught hypointense UCL (small arrows) and common flexor tendon origin (long arrows). Also notice normal common extensor tendon origin (curved arrows). In a case of recent elbow dislocation, corresponding 2D image (c) and 3D images (d,e) shows disruption of all of the above mentioned structures with similar arrows.

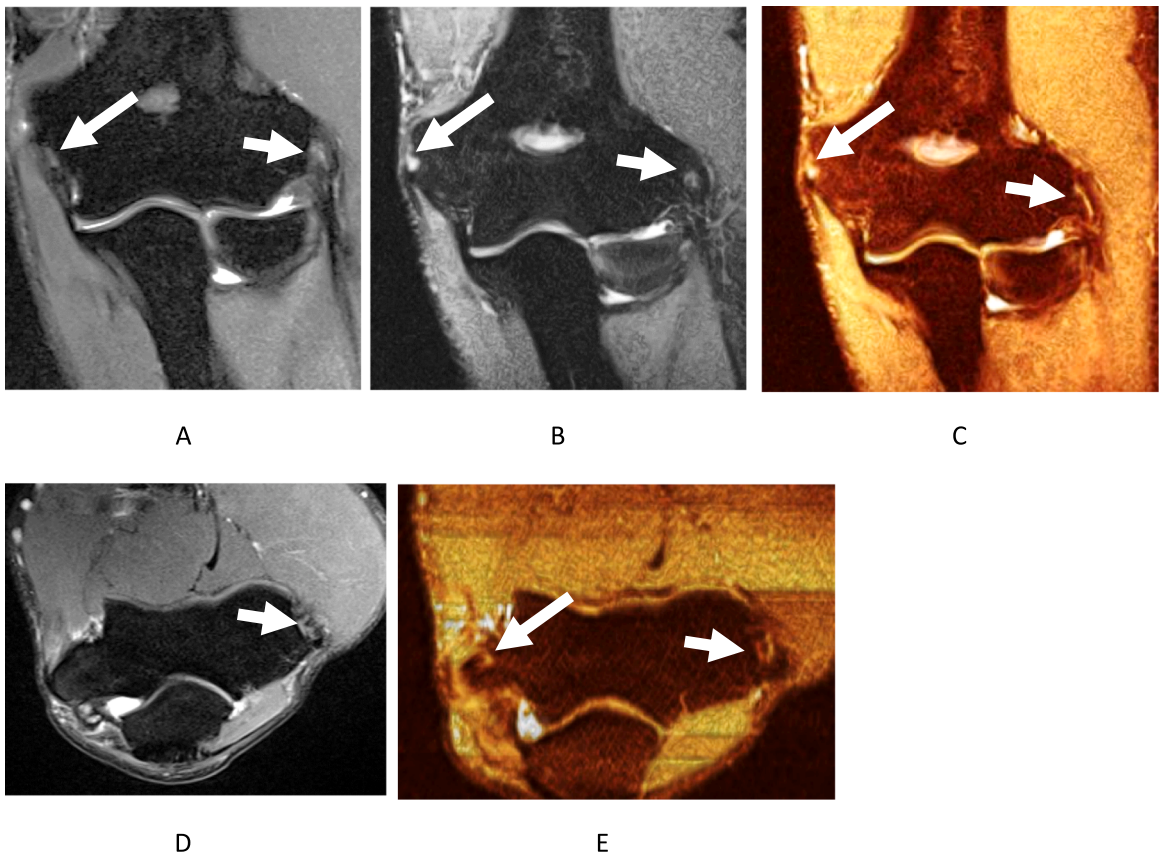

Fig. 5. Medial and lateral epicondylitis. Coronal 2D (a), coronal 3D (b,c), and axial 2D (d) and 3D (e) images show low grade partial tears of common flexor (small arrows) and extensor tendon (long arrows) origins. Notice axial more anatomic reconstruction from 3D imaging shows tears on both sides, better than 2D images (d,e).

Caipirinha technique (Siemens, Erlangen, Germany) and compressed SENSE (Phillips, Amsterdam, Netherlands). These improvements can additionally reduce imaging times to under 5 min while preserving image resolutions. The former stands for *Controlled Aliasing in Parallel Imaging* and it uses a group shifted *k*-space sampling patterns to reduce pixel aliasing and noise due to overlap on the reconstructed images. On the other hand, compressed SENSE (SENSitivity Encoding) sequence achieves faster acquisition times by using parallel imaging and under sampling of the k-space.

Elbow is divided in multiple anatomic compartments for a systematic assessment. Further discussion will focus on the role of high-resolution, particularly 3D MR imaging in various elbow pathologies, their clinical implications, and surgical perspectives that are critical for optimal and timely patient management.

3. Bones and joints

Radio-capitellar, ulno-trochlear and proximal radio-ulnar are important articulations around the elbow joint. While 2D MR imaging provides adequate evaluation of joint effusion, bone marrow edema and malalignments, 3D MR imaging has additional advantages, such as assessment of alignment in true anatomic planes generated along epicondyles, bone reconstruction without stair-step artifacts, improved assessment of synovial thickening, debris, and bodies with sharper resolution (Fig. 2) [10]. Fractures appear equally well on 2D and 3D MR imaging scans. Occult fracture of bone is seen as a focal hypointense line in the cloud of marrow edema and pseudoarthrosis are seen as fibrous articulation with subcortical cystic changes (Fig. 3). Finally, chondromalacia, cartilage fissuring, and flaps of osteochondral lesions are best seen on 3D imaging due to sharper images. The latter can facilitate pre-operative planning and aids in assessment of potential instability of such lesions.

4. Medial compartment

The important medial compartment structures include the ulnar collateral ligament and common flexor tendons.

4.1. Ulnar collateral ligament (UCL)

The UCL consists of three bundles (anterior, transverse, and posterior) and serves as the primary resistance against valgus stress [11]. The UCL is primarily evaluated on the coronal and axial planes and has a predominately low signal homogenous appearance that may include fat or inverted synovium proximally; the latter is normal and should not be mistaken for a tear (Fig. 1) [11,12]. Degenerative changes often appear

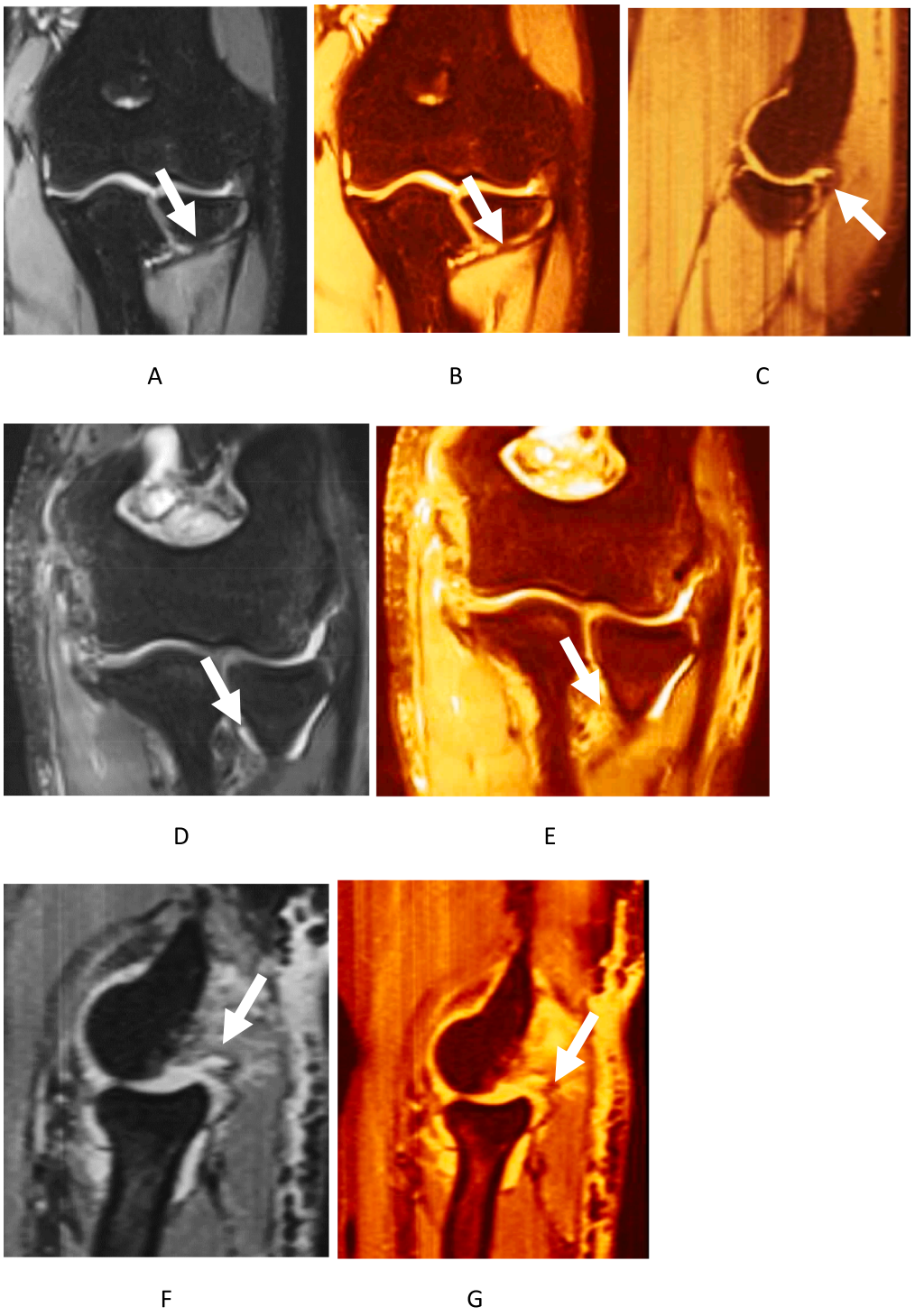

Fig. 6. LUCL- normal and abnormal appearances. Coronal 3D images (a-c) show normal taut LUCL (arrows). Coronal (d,e) and sagittal (f,g) images show disrupted LUCL with edema (arrow) and buckling, best seen on obliquely reconstructed sagittal images. Also note tears of common flexor and extensor tendons and UCL/RCL from recent elbow dislocation. The radius is subluxed posteriorly on the sagittal image.

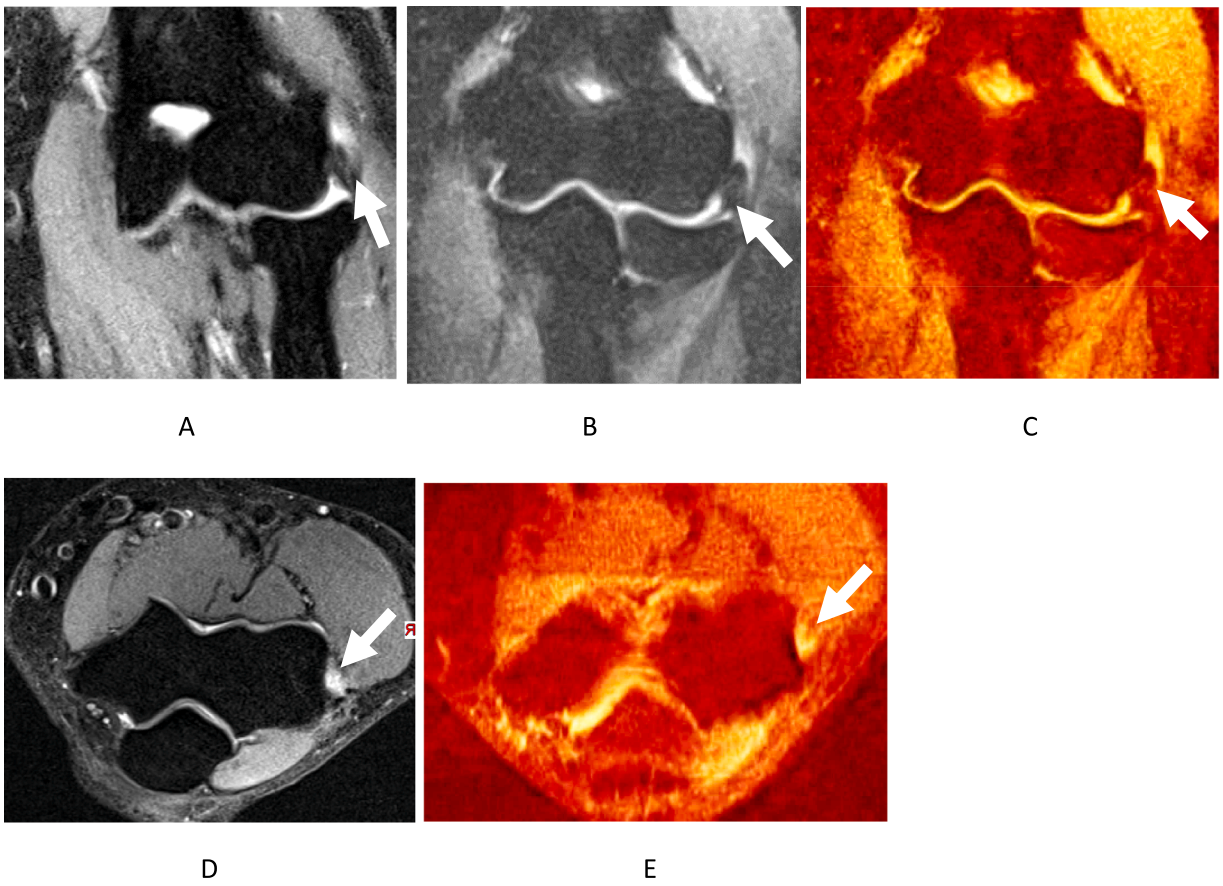

Fig. 7. Common extensor tear. Coronal 2d IMAGE (a) and 3D images (b,c,e) and axial 2D image (d) show full-thickness disruption/mass-avulsion of common extensor tendon origin with 1.0 cm retraction (arrows). Also note thickened and remodeled LCL.

as ligamentous thickening, thinning and/or fraying, which can be paired with an ossification or enteropathy at the humeral or ulnar attachment. Partial tear is often identified as focal discontinuity of the ligament fibers with or without partial thickness hyperintense fluid signal through the ligament. Distal tears result in a "T-sign" pattern characterized by linear-shaped fluid extending under the otherwise tight attachment of the UCL at the medial aspect of the coronoid process. It should be noted that the T-sign can be seen as a normal finding in children due to laxity of ligament [13]. Full-thickness tear shows complete discontinuity of the ligament with a fluid gap and laxity of the torn and/or retracted portions (Fig. 4). Associated regional hemorrhage and edema may be seen in the more-acute setting [11]. UCL reconstruction surgery is indicated for partial tears that have failed conservative management or complete tears in patients that want to continue competitive throwing. There are several modifications to the originally described technique, but all include drilling bone tunnels in the ulna and humerus with passage of a tendon graft in either a figure of eight fashion, tying the graft under tension to itself, or a docking technique which utilizes a single humeral bone tunnel and tying sutures over a bony bridge. MR imaging is also useful in post-surgical cases with persistent symptoms / instability or elbow dysfunction to illustrate the integrity or re-tears of a reconstructed UCL. 3D MR imaging reconstructions can outline the partial or complete re-tear along the length of the reconstruction.

4.2. Common flexor tendon (CFT)

The CFT aids the UCL in resisting valgus stress and originates from the anteromedial aspect of the medial epicondyle coursing distally to insert on the ulna as a uniformly low signal [14]. CFT injury is often due to overuse with valgus stress as well as repetitive wrist flexion and pronation. It typically occurs in overhead throwing motions and incorrect golf club swings resulting in tendinopathy, also known as medial epicondylitis [15]. It is graded as mild (with intermediate intrasubstance signal), moderate (thickening, fraying, and diffuse intermediate signal), and severe (diffuse almost fluid intense signal) [12]. These tendon changes are commonly associated with subjacent epicondylar stress changes such as subcortical edema, enthesopathy, and/or cystic changes. CFT tears demonstrate increased fluid-like signal or tendon discontinuation with less than 50% of the tendon thickness involvement considered as low-grade, $>$ 50% as high-grade, and full thickness aka mass avulsion. Associated soft tissue edema and hemorrhage is common in acute-subacute cases while enthesopathy and/or calcifications of the epicondylar attachment are frequent in chronic or acute on chronic cases. While partial injuries and tendinopathy are initially managed conservatively, 3D MRI isotropic images allow reconstruction of the tendon in an arbitrary plane along its long axis for improved visualization of a high-grade or full-thickness tear and the gap can be measured in different planes (Figs. 4,5). The imaging findings facilitate a decision to use primary repair or reconstruction of the tendon using auto- versus allografts.

5. Lateral compartment

5.1. Lateral collateral ligaments

The lateral collateral ligaments include the lateral ulnar collateral ligament (LUCL) which originates at the lateral epicondyle and courses posterior to the radial head-neck to insert on the lateral ulna, the radial collateral ligament (RCL) which originates at the anterior-lateral epicondyle, and the annular ligament which surrounds the radial head-neck

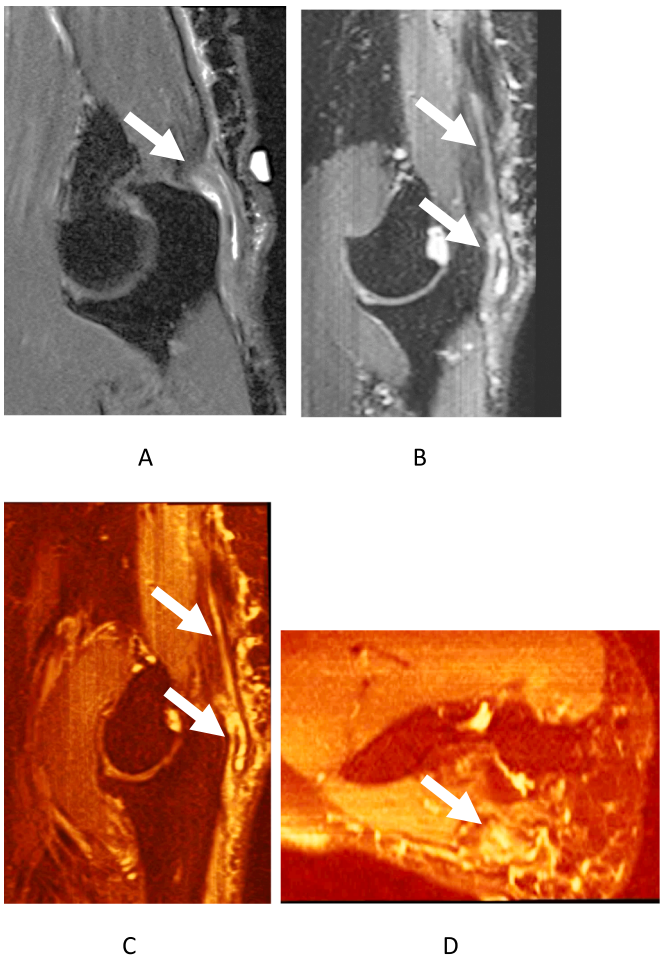

Fig. 8. Partial triceps tear. Sagittal 2D image (a) and sagittal and axial 3D images (b-d) show interstitial tears of triceps tendon (arrows) better defined on 3D images with intrasubstance extension proximally.

[16]. The LUCL is the primary restraint against posterolateral instability while the RCL resists varus stress. The annular ligament prevents distal radial displacement while pronating and supinating the forearm [5,17]. These ligaments are disrupted after elbow dislocation and can have associated cartilage injuries and fractures. On MR imaging, the ligament displays a uniform thickness and low signal intensity (Fig. 6), and a partial tear shows thinning / thickening of the ligament with increased signal intensity around and within the ligament while a complete tear shows discontinuity of the fibers with increased signal intensity [18]. Common patterns seen with lateral collateral ligament injury are as follows: RCL tears are often seen in conjunction with the common extensor tendon tear, e.g. in lateral epicondylitis. LUCL tears are associated with posterolateral joint space widening, and annular ligament tears will show radiocapitellar line disruption on sagittal radiographic view [12]. 3D MR imaging accurately outlines the ligament integrity by displaying the ligament along its long-axis (Figs. 4, 6). Associated cartilage injuries and intra-articular fractures are nicely depicted on MR imaging and can aid in surgical planning. If cartilage injury is minimal and fractures are without significant displacement, arthroscopic surgery can be performed to repair the lateral collateral ligament complex. Otherwise, an open repair may be performed to address concomitant fractures or cartilaginous injuries not suitable for arthroscopic surgery. Failed LCL repair may also be evaluated by 3D MR imaging to assess the repair and need for revision surgery.

5.2. *Lateral epicondylitis*

Lateral epicondylitis is often referred to as tennis elbow due to its frequent occurrence in tennis players. Although it most often occurs due to overuse injury in non-athletes, it is the most common condition affecting the lateral elbow[1]. Degeneration of the origin of the extensor carpi radialis brevis (ECRB) is frequently found to be at the core of this pathology followed by the anterior edge of the extensor digitorum communis origin and rarely the underside of the extensor carpi radialis longus or the origin of the extensor carpi ulnaris [19,20]. MR imaging is useful in the diagnosis and assessing the degree of injury, with normal tendons demonstrating a uniform low signal. Tendinosis is often seen on T1W or T2W images as an intermediate signal intensity within the tendon. Partial tendon tears exhibit high intensity on fluid sensitive sequences only seen partially across the tendon with diffuse thinning or thickening while complete tears exhibit a fluid signal intensity across the entire tendon or in between the proximal tendon and its humeral attachment aka mass avulsion (Figs. 5,7) [5]. Lateral Epicondylitis with and without tendon tearing is best treated conservatively with activity modifications, occupational therapy, and possible biologic injections. Surgery may be considered for those patients who fail prolonged nonoperative treatment. 3D MR imaging shows the accurate extent of the tendon tear with superior definition of tendon fibers in multiple planes facilitating pre- and post-operative assessments.

6. Posterior compartment

6.1. *Triceps tendon*

Triceps tendon injuries are rare with a male predominance and are the least common type of tendon injury around elbow, although other studies may suggest that these tears are more likely underdiagnosed as opposed to being a rare occurrence [21,22]. A partial tear in the triceps tendon is identified by small fluid filled defect in the distal triceps tendon with surrounding subcutaneous edema (Fig. 8) [23]. A complete tear shows a large fluid filled gap between the distal portion of the triceps tendon and its insertion (olecranon process) accompanied by fraying of tendon margins (heterogeneous signal) and retraction of the tendon, which is important to note for surgical intervention [23]. Partial tears including the posterior tendon may be difficult to visualize on the sagittal view because the torn portion of the tendon may be retracted into high position and the intact anterior portion may give the impression of a normal tendon [12]. Similar to the Achilles tendon, due to mechanism of injury being eccentric contraction in most cases, variable retraction of fibers may be elegantly depicted on 3D MR imaging (Fig. 9). It is essential to cover the field of view up to mid-upper arm in the settings of triceps and biceps tears in the sagittal plane on 2D or 3D MR imaging for optimal evaluations. The tendon quality and amount of retraction will aid the surgeon of possible need for tendon graft augmentation. Tendon repair can be performed using nonabsorbable sutures passed through the torn tendon and tied over bone utilizing bone tunnels or with use of suture anchors in the ulna.

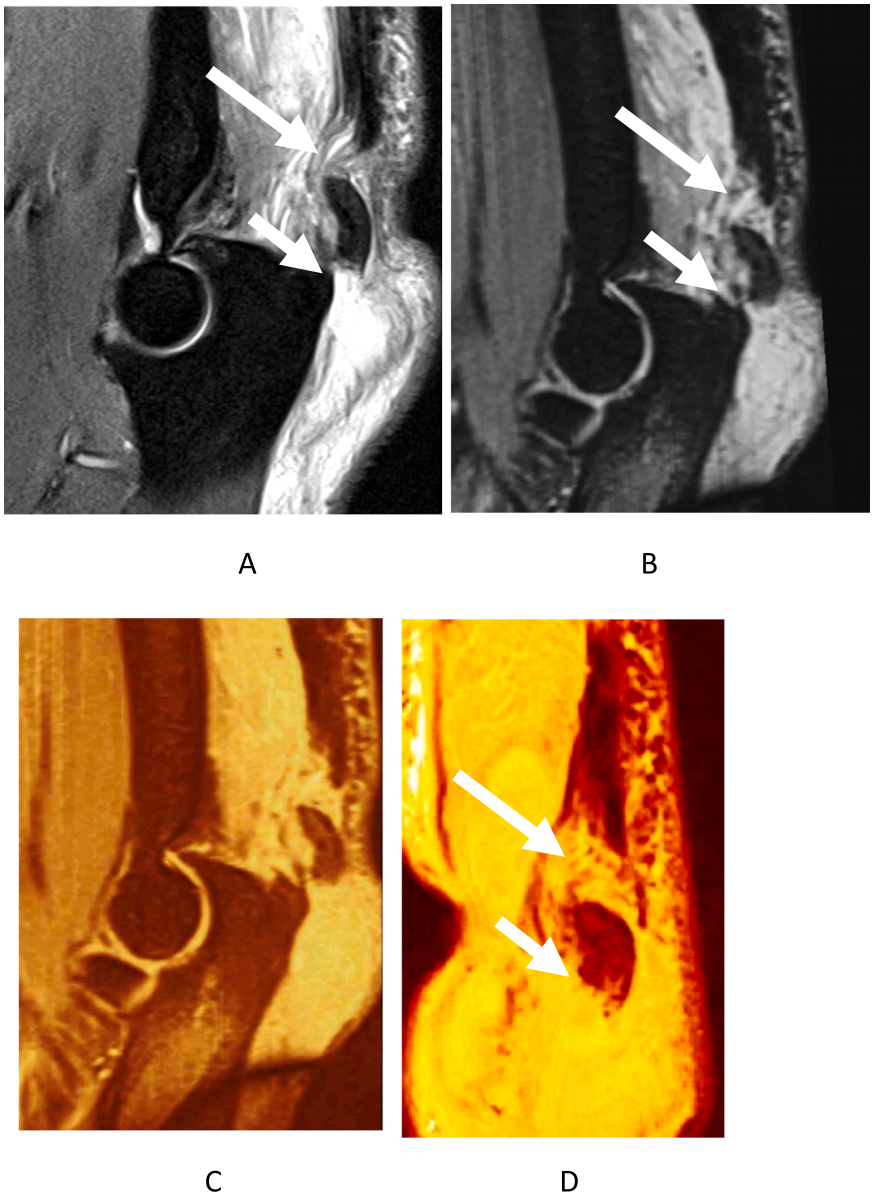

Fig. 9. Complete triceps tendon avulsion with tears. Sagittal 2D image (a), and sagittal 3D images (b,c) and coronal reconstruction along the triceps tendon (d) show bony avulsion of enthesophyte (small arrow) from the olecranon process, olecranon bursitis, surrounding hemorrhage and edema from recent injury, and near full-thickness triceps tears (long arrows).

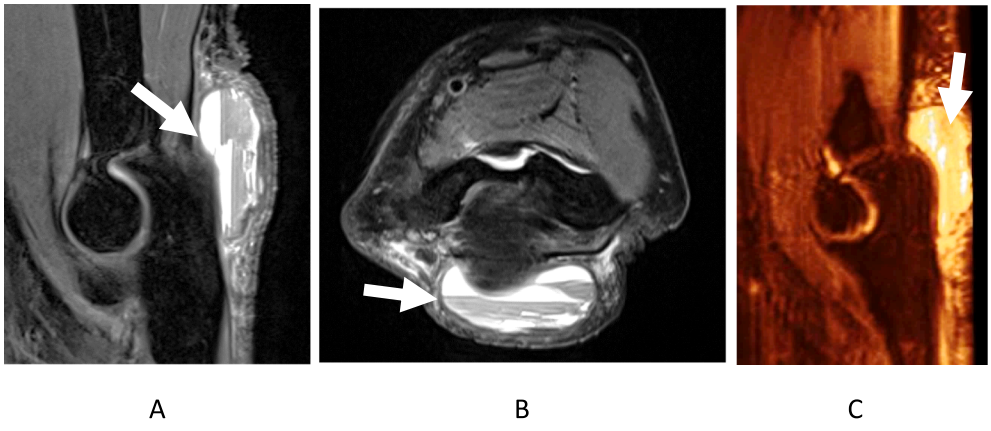

Fig. 10. Olecranon bursitis from recent injury and underlying anticoagulation. Sagittal and axial 2D images (a,b) and sagittal 3D image (c) show olecranon bursa distention with complexity- blood-fluid levels (arrows). The triceps tendon is intact.

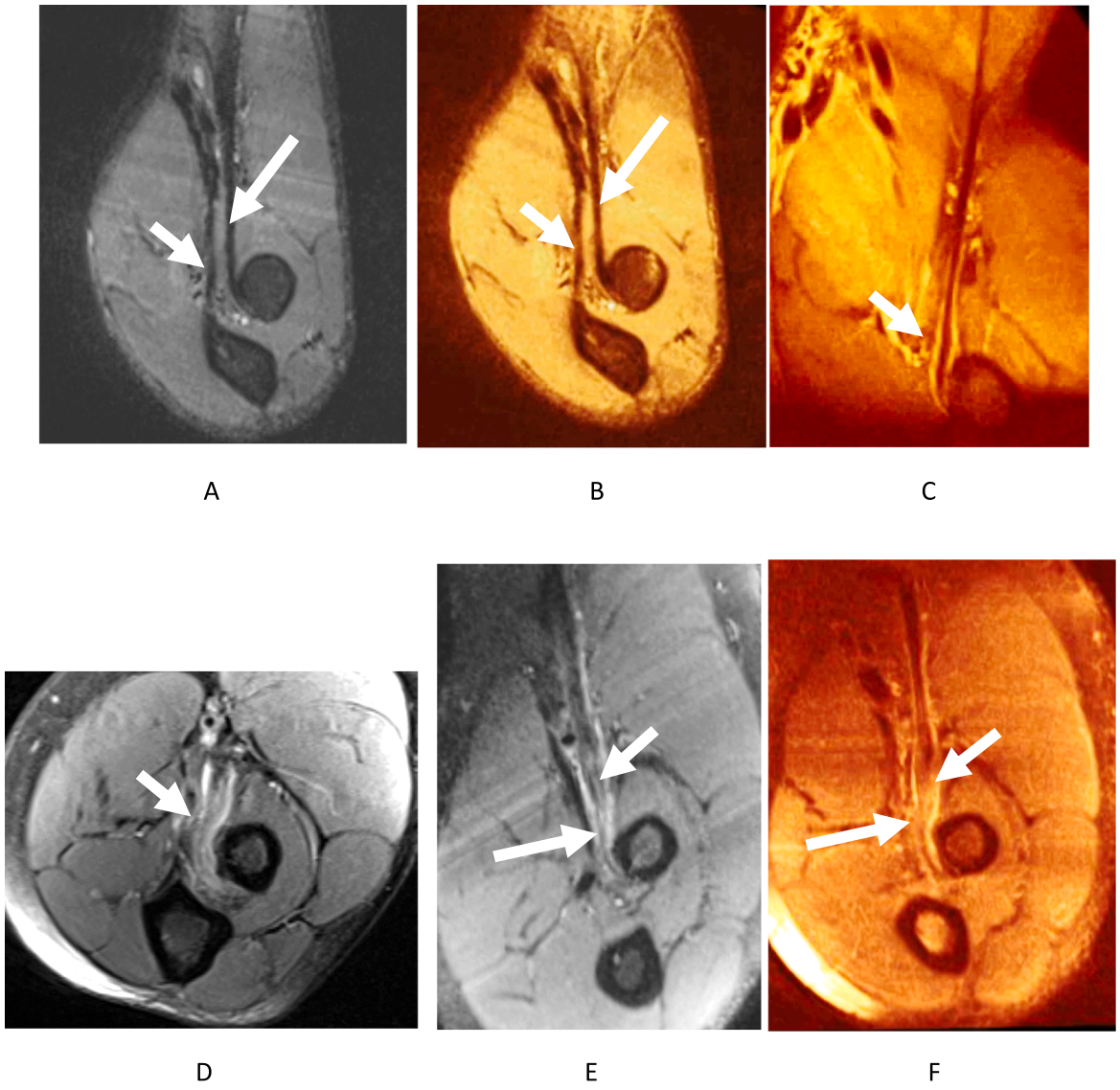

Fig. 11. Normal and abnormal biceps tendon. 3D imaging reconstruction of biceps (long arrows) and brachialis (short arrows) without the need for FABS (flexed elbow, abducted shoulder, forearm supinated) positioning (a,b). Notice mild bicipital-radial bursitis with grade I biceps sprain in a different case (c). Near-full thickness (high-grade) partial tear in an another patient on 2D axial (d) and 3D images (e,f). Notice better delineation of individual heads of biceps (long head-long arrows) with few fibers intact and torn-retracted short head (short arrows).

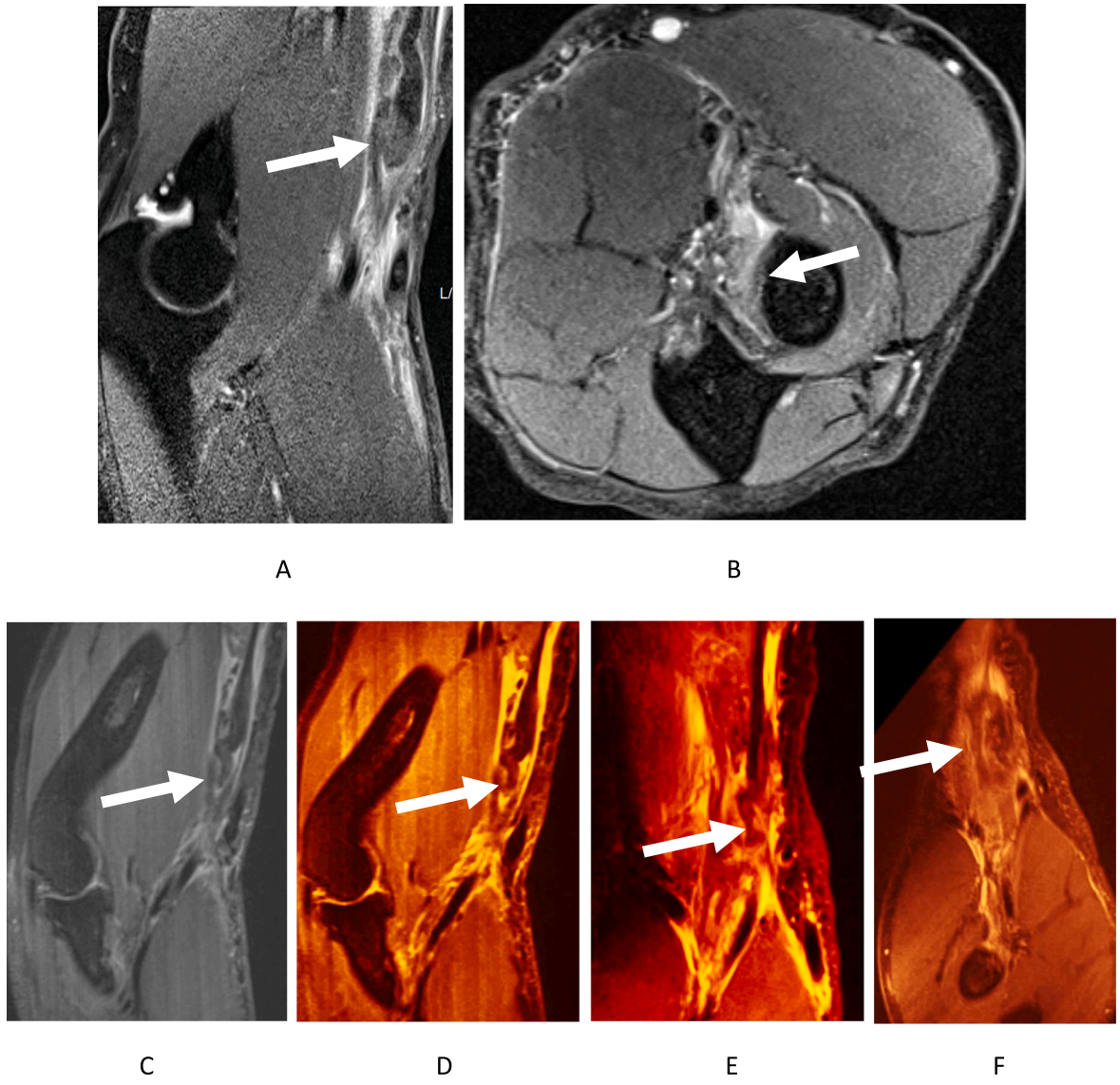

Fig. 12. Complete biceps and lacertus fibrosus tear with retraction. 2D MR images shows torn and retracted biceps tendon (arrows in a,b). 3D MR images reconstructed along the biceps tendon (arrows in c-f) demonstrate multiplanar depiction of the tendon retraction by up to 10 cm.

Olecranon fractures are often seen in high stress upper body dominant sports, and the non-displaced ones tend to appear as an irregular hypointense lines in a cloud of hyperintense edema [24]. Furthermore, olecranon bursitis is often, but not always associated with triceps tears and fractures (Fig. 10). It presents as a collection of fluid in the posterior subcutaneous tissues overlying the olecranon with/without thickened walls and gadolinium contrast enhancement. Gouty or septic bursitis can produce similar findings on MRI and clinical findings are useful for the diagnosis [16]. Bone erosions may be seen in either condition and dual energy CT may be helpful in finding gouty crystals.

7. Anterior compartment

Distal Biceps tendon injury accounts for 3–10% of all bicep tendon ruptures and is usually due to a single event often causing a tear near the distal insertion site (radial tuberosity) [25]. MR imaging is highly effective in detecting complete distal bicep tears as one study identified a sensitivity of 100% and partial distal bicep tears with a sensitivity of 59.1% [26]. 3D MR imaging can not only identify individual bundles of the biceps tendon and their tears but also is helpful in measurement of amount of tendon retraction (Figs. 11,12). Partial tears show fluid signal intensity of the distal tendon without complete discontinuation or

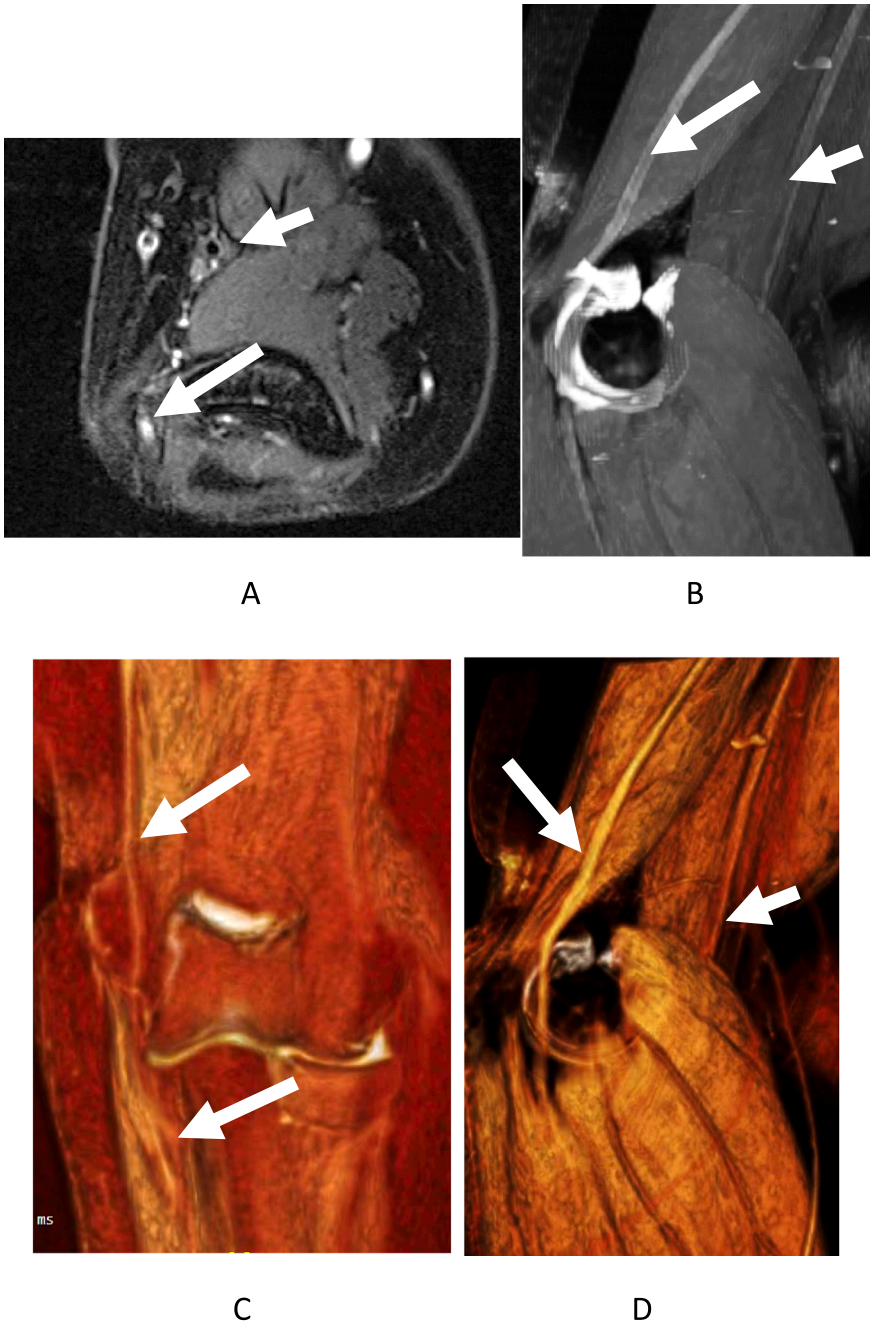

Fig. 13. Cubital tunnel syndrome. Axial 2D fsT2W image (a) and oblique sagittal and coronal reconstrcuted maximum intensity projection 3D images (b-d) shows abnormally hyperintense and enlarged ulnar nerve (long arrows) and normal isointense median nerve (small arrows).

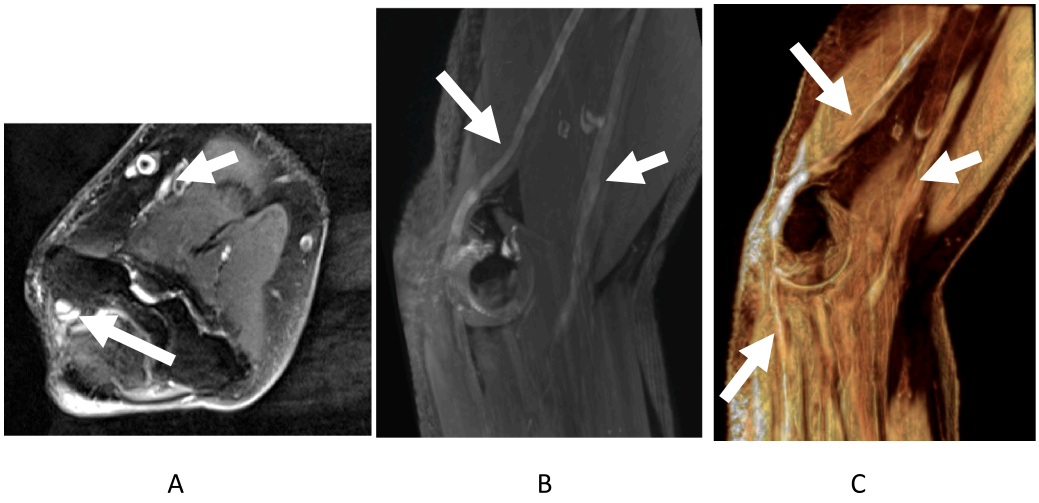

Fig. 14. Mononeuritis multiplex. Axial 2D fsT2W image (a) and oblique sagittal reconstrcuted maximum intensity projection 3D images (b,c) show diffusely abnormally hyperintense and enlarged ulnar nerve (long arrows) and median nerve (small arrows) consistent with clinical diagnosis of mononeuritis multiplex. Notice superimposed findings of cubital tunnel syndrome with focal enlargement of ulnar nerve at the tunnel.

retraction of the tendon [27]. Complete tears occur when the tendon is not visible at the radial tuberosity and there is proximal retraction of the tendon along with the distal tendon sheath being filled with edema or hemorrhage [27]. Retraction of the tendon may not occur if the bicipital aponeurosis remains intact [28]. Tendinopathy and/or tear of the biceps presents as an increased signal intensity, increased bone marrow edema of the radial tuberosity and bicipitoradial bursitis [26]. The brachialis muscle originates on the distal anterior humerus and inserts on the ulnar tuberosity. The brachialis serves as a powerful flexor of the elbow and appears as a low signal with uniform thickness [29]. Tendinopathies and tears of the brachialis follow a similar pattern to that of the biceps tendon [12]. In regard to biceps tendon repair surgery, the amount of retraction and tendon quality on MR imaging, will guide the surgeon for possible need of an additional incision to retrieve the proximal retracted biceps tendon in the upper arm as well as need for possible graft augmentation. MR imaging is also useful in post-repair or post-reconstruction assessment of the biceps tendon and finding re-tears.

7.1. Nerves

The three main nerves at the elbow are the median, radial, and ulnar nerves and their respective pathologies tend to be centered around nerve entrapment and compressive neuropathies and nerve injuries, which are accompanied by muscle denervation changes, with edema- like T2 signal, fatty degeneration, or atrophy, in the regional innervated muscles [12,30].

The radial nerve courses along the volar aspect of the elbow and through the lateral intermuscular septum and splits anterior to the lateral epicondyle. The portion that exits the supinator muscle is known as the posterior interosseous nerve (PIN) while the superficial branch is in between the supinator and brachioradialis muscles [16]. PIN compression tends to appear as an abnormal T2 hyperintensity that most often occurs at the arcade of Frohse (a low signal band at the proximal edge of the supinator muscle) [31,32]. Other sites of compressions of PIN and radial nerve are at the bicipital bursa and the distal edge of the supinator [33]. 3D MR imaging nicely demonstrates the nerve along its long-axis and its lesions, such as nerve injuries, mass lesion, and focal contour alterations from entrapments, thereby facilitating diagnosis and surgical planning.

The median nerve courses medial and parallel to the brachial artery [32]. Compression neuropathy of the median nerve tends to occur at several locations (between the humeral and ulnar heads of the pronator teres, the ligament of Struthers, the bicipital aponeurosis, and the fibrous arch of the flexor digitorum superficialis). 3D MRI can outline the anatomy including the anterior interosseous nerve in the oblique sagittal plane. Neuropathy shows as T2 hyperintense signal changes and contour changes of the nerves from entrapment or injury. The regional muscles may show denervation changes (edema and potential fatty atrophy) of pronator teres, flexor carpi radialis, palmaris longus, and flexor digitorum superficialis [32].

The ulnar nerve courses along the medial elbow behind the medial epicondyle and underneath the medial intermuscular septum. Neuropathy of the ulnar nerve is the most common nerve lesion of elbow and it most commonly occurs in the cubital tunnel (cubital tunnel syndrome, CTS). Etiologies of CTS include repeated elbow flexion activities, thickened Osborne ligament overlying the roof of the cubital tunnel, perineural fibrosis from prior injury or elbow fractures, tumor compression, and anconeus epitrochlearis muscle, an accessory muscle that can compress the ulnar nerve against the medial epicondyle or olecranon [32,34]. The MRI findings include ulnar nerve T2 hyperintensity approaching the adjacent ulnar collateral vessels, longitudinal extent of signal alteration, and enlargement or flattening of the ulnar nerve in the tunnel. It may be coupled with muscle denervation changes, manifesting as hyperintensity of the flexor carpi ulnaris and the ulnar portion of the flexor digitorum profundus on T2-weighted imaging [35]. While MR neurography and diffusion imaging are useful for ulnar neuropathy assessments, 3D anatomic MR imaging can outline the nerve along its long axis for depiction of primary and post-surgical

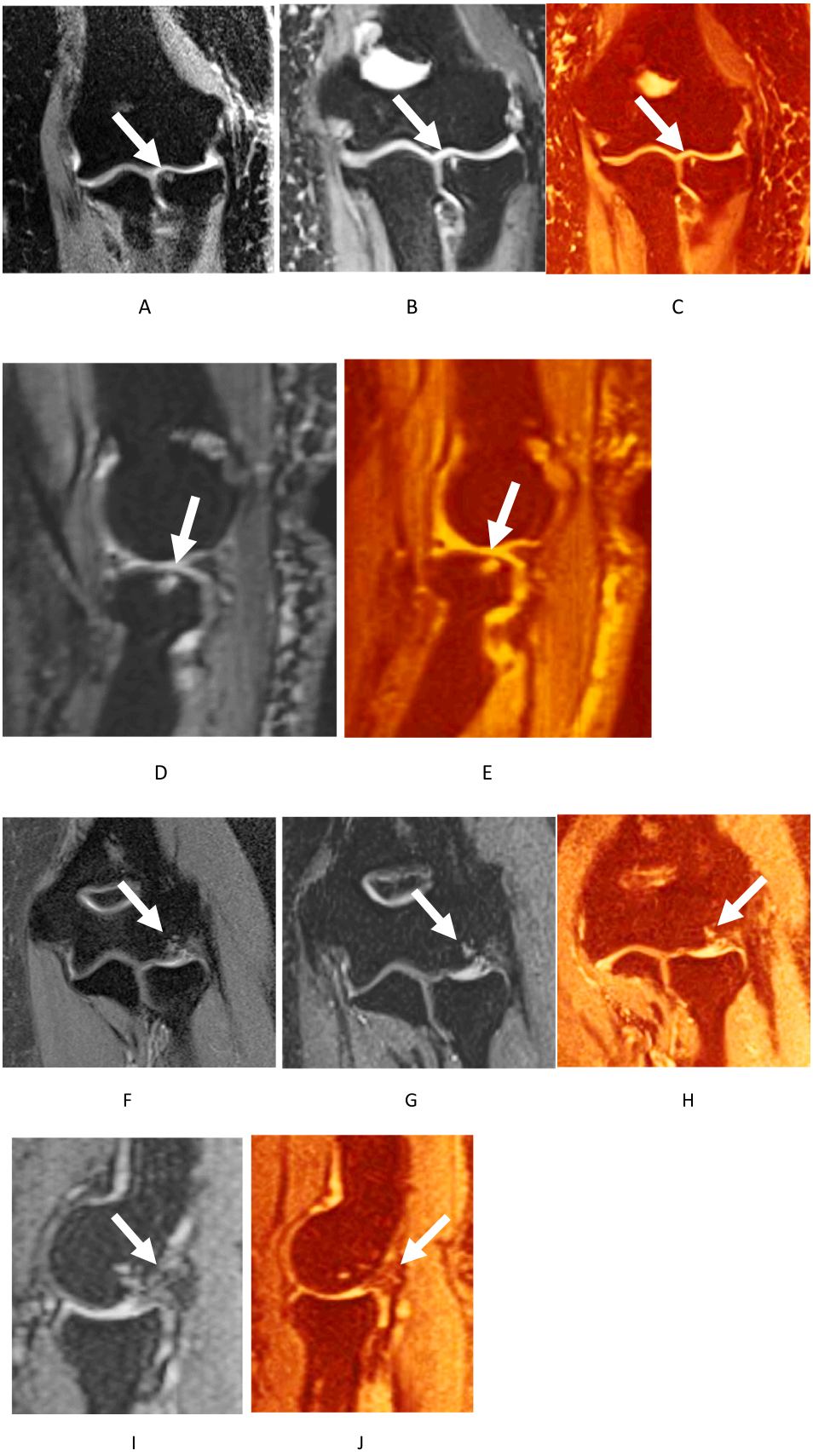

Fig. 15. True cartilage lesion versus pseudolesion. Coronal 3D fsIW (a) and coronal (b,c) images show small osteochondral lesion of medial aspect of the radial head with subchondral cyst (arrows). Notice focal cartilage loss at the posterior radial head on the sagittal images (d,e). In another case, a similar lesion at the capitellum (arrows in f-j), however at the traction site of LUCL origin with degeneration and thickening of the ligament (desmitis, arrows).

re-entrapments and inflammatory neuropathies (Figs. 13,14) [36].

One should remember pitfalls of 3D MRI. If not obtained isotropic, it can lead to stair-step artifacts. The imaging takes longer and is suboptimal on 1.5 T scanners unless above-described technical advancements are used. But 3D imaging helps mitigate partial-volume artifacts, aids in differentiating true cartilage lesions from pseudo-lesions and traction cysts (Fig. 15) and assists in tendon and ligament renderings along their long-axis for better display of anatomic lesions.

To conclude, MR imaging is a very useful adjunct modality for the diagnosis of elbow disorders. 3D MR imaging allows high-resolution assessment of the elbow derangements facilitating surgical planning and post-surgical evaluation.

Funding statement

This research did not receive any specific grant from funding agencies in the public, commercial, or not-for-profit sectors.

Ethical statement

All patients' images were obtained as part of retrospective IRB and informed consent was waived. University of Texas at Southwestern Medical Center Institutional Review Board guidelines were followed, and the images were reviewed in a HIPAA compliant manner.

Declaration of Competing Interest

The authors declare the following financial interests/personal relationships which may be considered as potential competing interests: Avneesh Chhabra serves as a consultant to ICON Medical and Treace Medical Concepts, Inc. Avneesh Chhabra also receives royalties from Jaypee and Wolters, and is a speaker for Siemens. Avneesh Chhabra is a medical advisor and recieved research grant from Image biopsy lab Inc. No other author has any disclosures or competing interests.

References

[1] M.A. Frick, N.S. Murthy, Imaging of the elbow: muscle and tendon injuries, Semin. Musculoskelet. Radiol. 14 (04) (2010) 430–437.
[2] S.F. Kane, J.H. Lynch, J.C. Taylor, Evaluation of elbow pain in adults, Am. Fam. Physician 89 (8) (2014) 649–657.
[3] G.P. Konin, L.N. Nazarian, D.M. Walz, US of the elbow: indications, technique, normal anatomy, and pathologic conditions, RadioGraphics 33 (4) (2013) E125–E147.
[4] K.J. Stevens, E.G. McNally, Magnetic resonance imaging of the elbow in athletes, Clin. Sports Med. 29 (4) (2010) 521–553.
[5] D. Binaghi, MR imaging of the elbow, Magn. Resonance Imag. Clin. North Am. 23 (3) (2015) 427–440.
[6] R. Kijowski, G.E. Gold, Routine 3D magnetic resonance imaging of joints, J. Magn. Reson Imag. 33 (4) (2011) 758–771.
[7] J.A. Carrino, W.B. Morrison, K.H. Zou, R.T. Steffen, W.N. Snearly, P.M. Murray, Noncontrast MR imaging and MR arthrography of the ulnar collateral ligament of the elbow: prospective evaluation of two-dimensional pulse sequences for detection of complete tears, Skeletal Radiol. 30 (11) (2001) 625–632.
[8] C. Sasiponganan, K. Yan, P. Pezeshk, Y. Xi, A. Chhabra, Advanced MR imaging of bone marrow: quantification of signal alterations on T1-weighted Dixon and T2-weighted Dixon sequences in red marrow, yellow marrow, and pathologic marrow lesions, Skeletal Radiol. 49 (4) (2020) 541–548.
[9] S. Kayfan, R. Hlis, P. Pezeshk, J. Shah, F. Poh, C. McCrum, A. Chhabra, Three-dimensional and 3-Tesla MRI morphometry of knee meniscus in normal and pathologic state, Clin. Anat. 34 (1) (2021) 143–153.
[10] V. Wadhwa, V. Malhotra, Y. Xi, S. Nordeck, K. Coyner, A. Chhabra, Bone and joint modeling from 3D knee MRI: feasibility and comparison with radiographs and 2D MRI, Clin. Imaging 40 (4) (2016) 765–768.
[11] J. Acosta Batlle, L. Cerezal, M.D. López Parra, B. Alba, S. Resano, J. Blázquez Sánchez, The elbow: review of anatomy and common collateral ligament complex pathology using MRI, Insights Imaging 10 (1) (2019) 43.
[12] A. Chhabra, M. Chalian, T. Soldatos, The Elbow, Musculoskeletal MRI Structured Evaluation: How to Practically Fill the Reporting Checklist Wolters Kluwer, Philadelphia (2014) 211–245.
[13] D.J. Lin, J.K. Kazam, F.S. Ahmed, T.T. Wong, Ulnar collateral ligament insertional injuries in pediatric overhead athletes: are MRI Findings predictive of symptoms or need for surgery? Am. J. Roentgenol. 212 (4) (2019) 867–873.
[14] D.M. Walz, J.S. Newman, G.P. Konin, G. Ross, Epicondylitis: pathogenesis, imaging, and treatment, RadioGraphics 30 (1) (2010) 167–184.
[15] M.C. Ciccotti, M.A. Schwartz, M.G. Ciccotti, Diagnosis and treatment of medial epicondylitis of the elbow, Clin. Sports Med. 23 (4) (2004) 693–705.
[16] A. Lombardi, A. Ashir, T. Gorbachova, M.S. Taljanovic, E.Y. Chang, Magnetic resonance imaging of the elbow, Pol. J. Radiol. 85 (2020) e440–e460.
[17] B.E. Fliegel, J. Ekblad, M. Varacallo, Anatomy, Shoulder and Upper Limb, Elbow Annular Ligament, StatPearls, Treasure Island ((FL)) (2021).
[18] M.A. Bredella, P.F. Tirman, R.C. Fritz, J.F. Feller, T.K. Wischer, H.K. Genant, MR imaging findings of lateral ulnar collateral ligament abnormalities in patients with lateral epicondylitis, Am. J. Roentgenol. 173 (5) (1999) 1379–1382.
[19] J.D. Saliman, C.F. Beaulieu, T.R. McAdams, Ligament and tendon injury to the elbow: clinical, surgical, and imaging features, Topics in Magn. Resonance Imag. 17 (5) (2006).
[20] R.P. Nirschl, F.A. Pettrone, Tennis elbow. The surgical treatment of lateral epicondylitis, J. Bone Joint Surg. Am. 61 (6a) (1979) 832–839.
[21] C. Stucken, M.G. Ciccotti, Distal biceps and triceps injuries in athletes, Sports Med. Arthrosc. Rev. 22 (3) (2014) 153–163.
[22] M.C. Koplas, E. Schneider, M. Sundaram, Prevalence of triceps tendon tears on MRI of the elbow and clinical correlation, Skeletal Radiol. 40 (5) (2011) 587–594.
[23] R. Kijowski, M. Tuite, M. Sanford, Magnetic resonance imaging of the elbow. Part II: abnormalities of the ligaments, tendons, and nerves, Skeletal Radiol. 34 (1) (2005) 1–18.
[24] D.R. Wenzke, MR imaging of the elbow in the injured athlete, Radiologic Clin. North Am. 51 (2) (2013) 195–213.
[25] R. Thornton, G.M. Riley, L.S. Steinbach, Magnetic resonance imaging of sports injuries of the elbow, Topics Magn. Resonance Imag. 14 (1) (2003).
[26] A. Festa, P.J. Mulieri, J.S. Newman, D.J. Spitz, B.M. Leslie, Effectiveness of magnetic resonance imaging in detecting partial and complete distal biceps tendon rupture, J. Hand Surgery 35 (1) (2010) 77–83.
[27] F.S. Falchook, M.B. Zlatkin, G.E. Erbacher, J.S. Moulton, G.S. Bisset, B.J. Murphy, Rupture of the distal biceps tendon: evaluation with MR imaging, Radiology 190 (3) (1994) 659–663.
[28] M.L. Chew, B.M. Giuffrè, Disorders of the distal biceps brachii tendon, RadioGraphics 25 (5) (2005) 1227–1237.
[29] M.A. Plantz, B. Bordoni, Anatomy, Shoulder and Upper Limb, Brachialis Muscle, StatPearls, Treasure Island ((FL)) (2021).
[30] B. Chirdeep, K. Batra, Elbow MRI, eMedicine (2020).
[31] N. Faridian-Aragh, M. Chalian, T. Soldatos, G.K. Thawait, E.G. Deune, A. J. Belzberg, J.A. Carrino, A. Chhabra, High-resolution 3T MR neurography of radial neuropathy, J. Neuroradiol. 38 (5) (2011) 265–274.
[32] T.T. Miller, W.R. Reinus, Nerve entrapment syndromes of the elbow, forearm, and wrist, Am. J. Roentgenol. 195 (3) (2010) 585–594.
[33] P. Tsai, D.R. Steinberg, Median and radial nerve compression about the elbow, JBJS 90 (2) (2008).
[34] D.B. Husarik, N. Saupe, C.W.A. Pfirrmann, B. Jost, J. Hodler, M. Zanetti, Elbow nerves: MR findings in 60 asymptomatic subjects—normal anatomy, variants, and pitfalls, Radiology 252 (1) (2009) 148–156.
[35] A. Agarwal, A. Chandra, U. Jaipal, N. Saini, Imaging in the diagnosis of ulnar nerve pathologies-a neoteric approach, Insights Imag. 10 (1) (2019), 37-37.
[36] L. Zhao, G. Wang, L. Yang, L. Wu, X. Lin, A. Chhabra, Diffusion-weighted MR neurography of extremity nerves with unidirectional motion-probing gradients at 3 T: feasibility study, AJR Am. J. Roentgenol. 200 (5) (2013) 1106–1114.